

# In Situ Observation of the Crystalline Transformation from Cellulose III<sub>I</sub> to I<sub>β</sub>

Masahisa Wada\*

Department of Biomaterials Science, Graduate School of Agricultural and Life Sciences,  
The University of Tokyo, Yayoi 1-1-1, Bunkyo-ku Tokyo 113-8657, Japan

Received July 31, 2000; Revised Manuscript Received February 17, 2001

**ABSTRACT:** An oriented, crystalline film of cellulose I was transformed into cellulose III<sub>I</sub> by supercritical ammonia treatment. These oriented, crystalline cellulose III<sub>I</sub> films were converted into cellulose I<sub>β</sub> crystalline film by heating in air for 1 h at 230 °C. This transformation process, from cellulose III<sub>I</sub> to I<sub>β</sub>, was studied by differential scanning calorimetry and X-ray diffraction methods. During the heating, an endothermic peak was observed at 200 °C. This suggests that some hydrogen bonds are broken, which might trigger the transformation from cellulose III<sub>I</sub> to I<sub>β</sub> at this temperature. Analysis of the X-ray diffraction results revealed that cellulose III<sub>I</sub> transforms into I<sub>β</sub> in the temperature range 200–217 °C. At 217 °C, the intrasheet and intersheet distances between cellulose chains in both the cellulose III<sub>I</sub> and I<sub>β</sub> crystalline phases are almost identical. Thus, we propose a mechanism account for the cellulose III<sub>I</sub> transformation into I<sub>β</sub> by shear of the hydrogen-bonded cellulosic sheets in the *bc*-plane.

## Introduction

Cellulose I is a natural form of cellulose, and there are two crystalline polymorphs: I<sub>α</sub> and I<sub>β</sub>.<sup>1,2</sup> The structures of cellulose I<sub>α</sub> and I<sub>β</sub> are assigned to the triclinic and monoclinic crystalline systems, respectively.<sup>3</sup> The I<sub>β</sub> phase is considered to be more stable than the I<sub>α</sub> phase, because I<sub>α</sub> transforms into I<sub>β</sub> after hydrothermal treatment.<sup>4</sup> Furthermore, Debzi et al.<sup>5</sup> reported that most of the I<sub>α</sub> phase could be converted into I<sub>β</sub> under an atmosphere of helium. This suggests that the important factor is temperature and not existence of water for the transformation between cellulosic polymorphs.

Another polymorph, cellulose III<sub>I</sub>, is obtained by treatment of cellulose I in liquid ammonia<sup>6,7</sup> or various amines<sup>8–10</sup> followed by removal of these reagents. Cellulose III<sub>I</sub> can be reverse transformed into cellulose I<sub>β</sub> by treatment in hot water.<sup>11–14</sup> The above finding by Debzi et al.<sup>5</sup> was the motivation to check whether the cellulose III<sub>I</sub> transformed into I<sub>β</sub> by heating without water, based on the reasoning that if the conversion occurs by heating alone, it would be possible to observe in situ the phase transformation process by physical means.

Recently, Nishiyama et al.<sup>15</sup> developed a way to make uniaxial oriented cellulose I films from crystalline cellulose samples. Also, Yatsu et al.<sup>16</sup> prepared crystalline cellulose III samples with supercritical ammonia. Using these methods, oriented crystalline cellulose III<sub>I</sub> films were prepared using a supercritical ammonia treatment on oriented cellulose I films. Thereafter, by using the prepared films, cellulose III<sub>I</sub> was found to be transformed into cellulose I<sub>β</sub> by heat treatment. In this report, the result of monitoring the phase transformation process by differential scanning calorimetry (DSC) and X-ray diffraction are described, and a phase transformation mechanism is proposed.

## Experimental Section

**Materials.** The sample used in this study was crystalline cellulose from green marine alga *Cladophora*. The alga sample was repeatedly purified with 5% KOH and 0.3% NaClO<sub>2</sub> solution according to the method previously reported.<sup>17</sup> The purified sample was homogenized into small fragments using a double-cylinder type homogenizer, and these fragments were treated with 65% sulfuric acid at 70 °C for 30 min with continuous stirring. The samples were washed with deionized water by successive dilution and centrifugation at 3200g for 5 min until the supernatant became turbid. The turbid supernatant was collected and concentrated by a high-speed centrifuge at 18 800g for 40 min and further dispersed into a small amount of distilled water. The concentrated suspension was sonicated with a rod-type sonicator for 1 min. The suspension was finally treated by placing it in contact with a mixed-bed ion-exchange resin.

Thin films of cellulose microcrystals with random orientation were obtained by casting the suspension on a glass plate followed by drying in air for several days. The films were further dried at 50 °C for 24 h and stored in a desiccator over P<sub>2</sub>O<sub>5</sub> until used.

Oriented films of cellulose microcrystals were prepared from the suspension by the shearing method as previously reported.<sup>15</sup> In short, the suspension with a small amount of sulfuric acid was put into a glass vial, and the vial was then kept horizontal and rotated around its center. After a few hours, the gel layer attached on the inner surface of the glass vial was dried into a film by repeated treatment of rinsing with ethanol and drying with a warm air flow. The films of oriented microcrystals were further dried at 105 °C for 8 h and stored in a desiccator over P<sub>2</sub>O<sub>5</sub> until used.

**Supercritical Ammonia Treatment.** The films were placed in a steel pressure vessel, which was cooled in a dry ice/methanol bath. By introducing the NH<sub>3</sub> gas into the cooled vessel, the sample was immersed in liquid NH<sub>3</sub>. The vessel was hermetically sealed and maintained at room temperature for 30 min. The vessel was then heated at 140 °C, which is above the critical temperature of ammonia: 132.5 °C, for 1 h in an oil bath. After the vessel was taken out of the oil bath, the NH<sub>3</sub> gas was immediately vented. The treated samples were thoroughly washed with dry methanol and dried under high vacuum at 50 °C.<sup>16,18,19</sup> Oriented cellulose III<sub>I</sub> films with high degree of crystallinity were obtained.

\* Further correspondence should be addressed to: Masahisa Wada, H. H. Wills Physics Laboratory, University of Bristol, Royal Fort, Tyndall Avenue, Bristol BS8 1TL, U.K. Fax +44-117-925-5624, e-mail wadam@sbp.fpa.u-tokyo.ac.jp.

**X-ray Fiber Diffraction.** The oriented cellulose III<sub>I</sub> films were heated at 230 °C in air for 1 h. X-ray fiber diffraction diagrams of the films before and after heat treatment were obtained using a vacuum camera mounted on a Rigaku RU-200BH rotating anode X-ray generator. Ni-filtered Cu K $\alpha$  radiation ( $\lambda = 0.154\ 18\ \text{nm}$ ) generated at 50 kV and 100 mA was used. These samples were irradiated using an incident X-ray beam that was collimated by a pinhole 0.3 mm diameter, and the fiber diffraction patterns were recorded on Fuji film imaging plates (BAS-IP SR 127). The camera length was calibrated using NaF ( $d = 0.231\ 66\ \text{nm}$ ).

**FT-IR Spectroscopy.** The randomly oriented thin films treated with ammonia were heated at 230 °C in air for 1 h. FT-IR spectra of the films before and after heat treatment were obtained using a Nicolet Magna 860. All spectra were recorded with an accumulation of 64 scans, resolution of  $4\ \text{cm}^{-1}$ , in the range from 4000 to  $400\ \text{cm}^{-1}$ .

**DSC Measurements.** DSC was performed with a Perkin-Elmer Pyris1. About 3 mg of ammonia treated cellulose sample was sealed in an aluminum pan. The sample was then heated from 150 to 250 °C at a rate of  $5\ ^\circ\text{C}/\text{min}$ . After holding the temperature at 250 °C for 5 min, the samples were cooled at a rate of  $-5\ ^\circ\text{C}/\text{min}$  to 150 °C.

**X-ray Diffractometry under Heat Treatment.** Equatorial X-ray diffraction profiles were obtained using a sample heating holder and a position-sensitive proportional counter (PSPC) mounted on a Rigaku RINT 2200 goniometer. Ni-filtered Cu K $\alpha$  radiation ( $\lambda = 0.154\ 18\ \text{nm}$ ) generated at 36 kV and 50 mA was collimated by a pinhole of 1.0 mm diameter. The oriented cellulose III<sub>I</sub> film sample was positioned at the center of the goniometer as the film surface was perpendicular to the incident X-rays ( $\theta = 90^\circ$ ), and the PSPC was placed to cover the range of  $2\theta$  from  $8^\circ$  to  $30^\circ$ . After the sample was placed in the heating holder, the atmosphere in the holder was completely replaced with helium. The diffraction pattern was recorded for the initial sample at room temperature. The sample was heated to a specific temperature at a rate of  $5\ ^\circ\text{C}/\text{min}$  and kept there for 2 min while the diffraction pattern was recorded. The measurement and heating process was repeated up to 250 °C. After holding the temperature at 250 °C for several minutes, the sample was cooled to room temperature at a rate of  $-5\ ^\circ\text{C}/\text{min}$ . Finally, the pattern at room temperature was recorded.

## Results and Discussion

An X-ray fiber diagram of the supercritical ammonia treated film is shown in Figure 1A. The pattern is typical of highly crystalline cellulose III<sub>I</sub> with two strong reflections (a) and (b) located on the equator at  $d = 0.759$  and  $0.427\ \text{nm}$  and an intense reflection (c) on the meridian at  $d = 0.518\ \text{nm}$ . According to a one chain unit cell with  $P2_1$  symmetry,<sup>20,21</sup> reflection (a) was indexed as 010, (b) was the overlapping of the two reflections 100 and 110, and (c) was 002.

Figure 1B is an X-ray fiber diagram of the annealed film of Figure 1A at 230 °C for 1 h. This pattern, the resolution of which is poorer than that of the initial cellulose III<sub>I</sub>, closely resembles the fiber diagram of ramie cellulose.<sup>22</sup> Three crystalline reflections (d), (e), and (f) with broader width appeared on the equator at  $d = 0.597$ ,  $0.538$ , and  $0.394\ \text{nm}$ , respectively. A weak reflection (g), which was comparable with intense reflection (c) of cellulose III<sub>I</sub>, was observed on the meridian. Furthermore, all reflections in the diagram were indexed according to the I $\beta$  monoclinic unit cell,<sup>3,22</sup> there being no observed characteristic I $\alpha$  reflection. Therefore, the diagram was of cellulose I $\beta$ , the same as ramie, indicating that cellulose III<sub>I</sub> transformed into cellulose I $\beta$  by heat treatment without water.

To confirm the X-ray fiber diffraction results, FT-IR measurements of thin films were performed. Figure 2

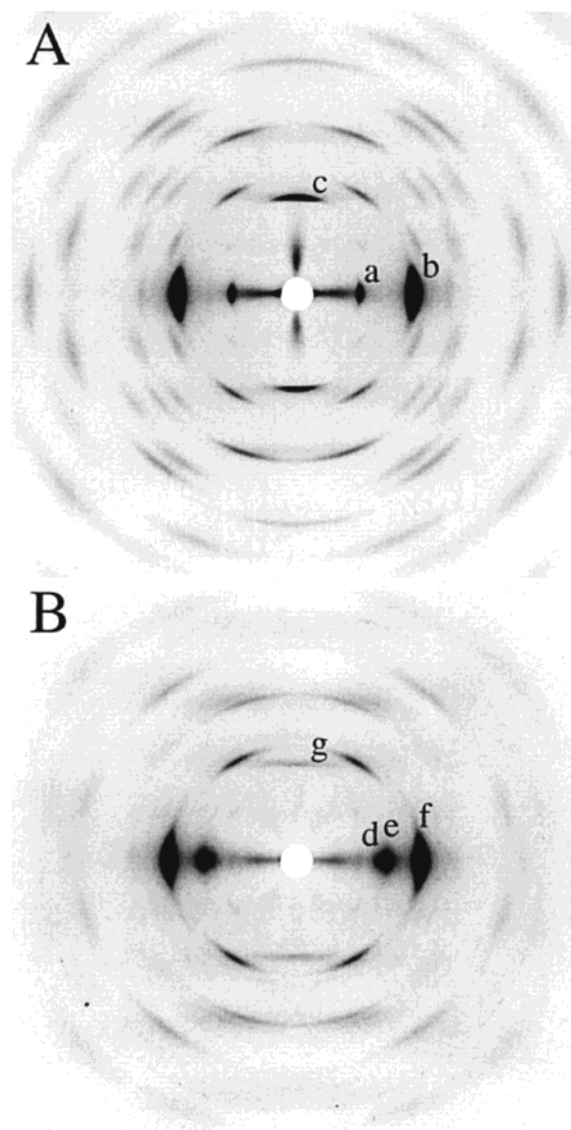


**Figure 1.** X-ray fiber diagrams of crystalline cellulose III<sub>I</sub> (A) and heat-treated cellulose, held at 230 °C for 1 h (B). Diagram B is a typical cellulose I $\beta$  pattern.

shows the FT-IR spectra of before (A) and after (B) heat treatment of cellulose III<sub>I</sub> films in the OH stretching region recorded with a resolution of  $4\ \text{cm}^{-1}$ . Only three bands, one sharp band at  $3480\ \text{cm}^{-1}$  and two broad bands at  $3300$  and  $3150\ \text{cm}^{-1}$ , exist in the spectra of cellulose III<sub>I</sub>. On the other hand, the annealed spectrum is the same as that of *Halocynthia*, ramie, and cotton cellulose, which are I $\beta$  type cellulose. In accordance with Sugiyama et al.,<sup>17</sup> the bands at  $3240$  and  $3270\ \text{cm}^{-1}$  were assigned to I $\alpha$  and I $\beta$ , respectively. In the spectrum of the annealed film, the band at  $3270\ \text{cm}^{-1}$  is clearly observed, but no band is present at  $3240\ \text{cm}^{-1}$ . Thus, the annealed sample is cellulose I $\beta$ . From the FT-IR results, we confirmed that the III<sub>I</sub> to I $\beta$  transformation was induced by heat treatment.

The above X-ray and FT-IR results were the motivation to monitor the crystalline phase transformation process. First, the monitoring process was undertaken by in situ DSC measurements. Figure 3 is a DSC thermogram of cellulose III<sub>I</sub> for the heating and cooling processes. In the heating process, an endothermic peak, whose onset was  $195\ ^\circ\text{C}$ , was observed at  $200\ ^\circ\text{C}$ .<sup>23</sup> This

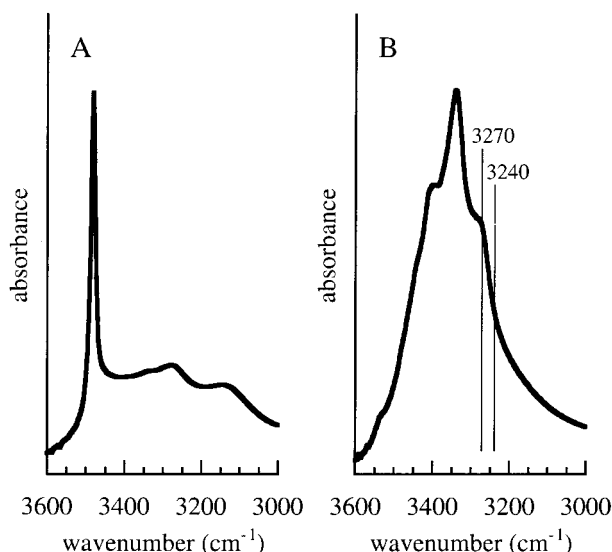


**Figure 2.** FT-IR spectra in the OH stretch region of cellulose III<sub>I</sub> (A) and cellulose I<sub>β</sub> (B), which was converted from the cellulose III<sub>I</sub> sample by heat treatment at 230 °C for 1 h.

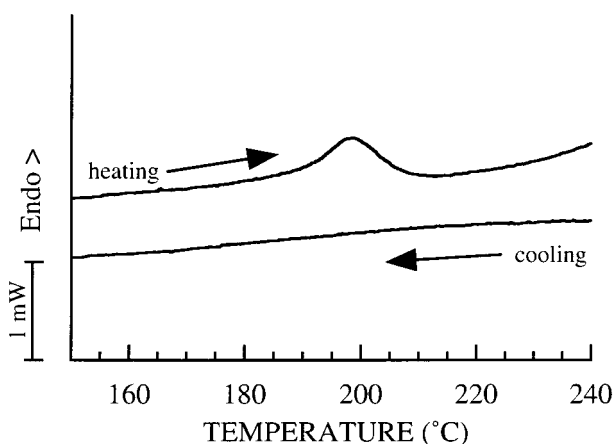


**Figure 3.** DSC thermogram of the crystalline phase transition process from cellulose III<sub>I</sub> to cellulose I<sub>β</sub>.

result indicates that release of some hydrogen bonding may occur at this temperature. Above this temperature, cellulose chains may move more flexibly to relax into the more stable I<sub>β</sub> structure. With increasing temperature, thermal vibration of the molecular chains increases, and as a result, the amount of transformation to the I<sub>β</sub> phase would be expected to increase. However, in the cooling process no peak was observed. After DSC measurements, the sample was removed from the pan and X-ray diffraction undertaken. The observed diffraction profile was that of cellulose I<sub>β</sub>, suggesting that the cellulose III<sub>I</sub> completely transformed into I<sub>β</sub> by this thermal treatment.

To observe in situ the crystalline phase transition from cellulose III<sub>I</sub> to I<sub>β</sub>, X-ray diffraction was performed at specific temperatures. Figure 3 shows the equatorial X-ray diffraction profiles for the crystalline phase transformation process from cellulose III<sub>I</sub> to I<sub>β</sub>. Three equatorial reflections of cellulose III<sub>I</sub>, symbolized 1, 2, and 3, which were indexed at 010, 100/110, and 110, respectively, were observed at room temperature before heating. As the sample was heated to 192 °C, peak 2 shifted noticeably to smaller angles because of thermal expansion, while peaks 1 and 3 shifted only to a small extent. When the temperature increased to 200 °C, the

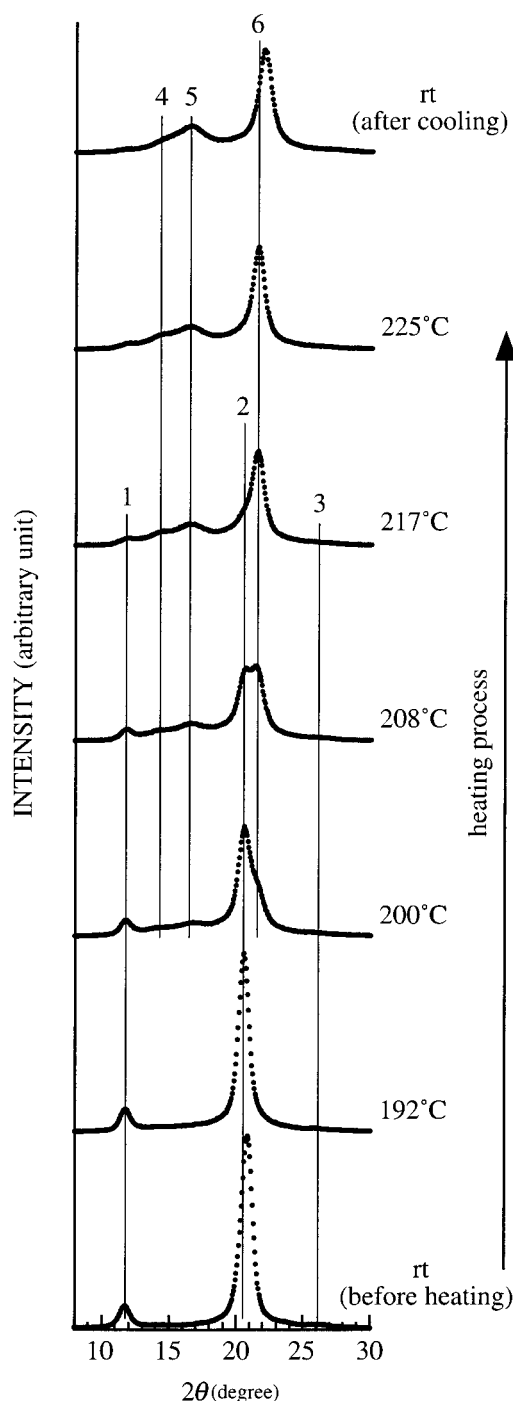


**Figure 4.** Equatorial X-ray diffraction profiles in the crystalline phase transformation process from cellulose III<sub>I</sub> to I<sub>β</sub> at specific temperatures in an atmosphere of helium.

three peaks (4, 110; 5, 110; 6, 200) that correspond to cellulose I<sub>β</sub> appeared, and the intensity of peaks 1, 2, and 3 assigned to cellulose III<sub>I</sub> diminished. At 208 °C, the cellulose III<sub>I</sub> and I<sub>β</sub> phases were approximately 50:50. The cellulose III<sub>I</sub> phase was almost completely converted into cellulose I<sub>β</sub> phase at 225 °C. After heating to 250 °C, the sample was cooled to room temperature. Although the peaks shifted to wider angles by thermal shrinkage, the profiles remained as the I<sub>β</sub> pattern. These X-ray results indicate that cellulose III<sub>I</sub> directly transformed into I<sub>β</sub> at 200–217 °C during the heating process.

To consider how the transformation from cellulose III<sub>I</sub> to I<sub>β</sub> proceeded, peak fitting of the X-ray diffraction



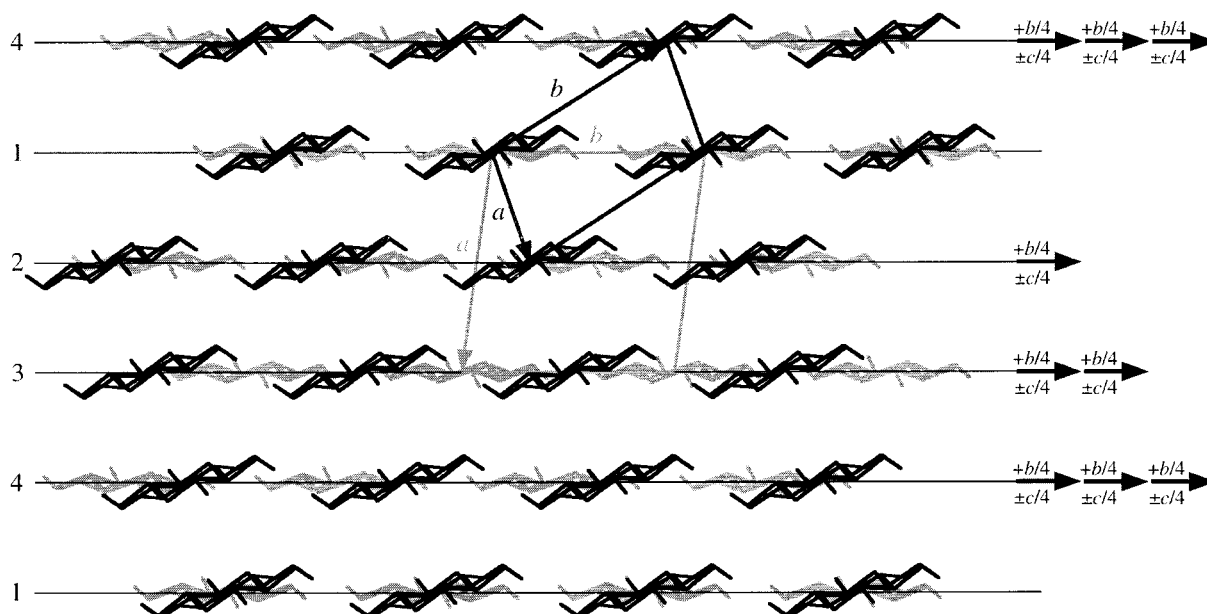


**Figure 5.** Schematic representation of the crystalline transformation from cellulose III<sub>I</sub> to I<sub>β</sub>. The black and gray lines represent the *ab* projection (*c*-axis projection) of the unit cell and cellulose chains of cellulose III<sub>I</sub> and I<sub>β</sub> at 217 °C, respectively. The hydrogen-bonded cellulose molecular sheets (1, 2, 3, and 4) translate  $+b/4$  to the *b*-axis direction of the I<sub>β</sub> phase and  $+c/4$  progressively (or  $-c/4$  progressively) to the *c*-axis direction.

profile at 217 °C was undertaken. In the fitting process, a fifth-degree polynomial function for a background profile was used, a pseudo-Voigt function for each crystalline reflection,<sup>24</sup> and the Levenberg–Marquardt algorithm applied. The *d*-spacings of each reflection were  $d_{010}$  III<sub>I</sub> (1) = 0.752 nm,  $d_{100}$  III<sub>I</sub>/ $d_{110}$  III<sub>I</sub> (2) = 0.433 nm,  $d_{110}$  III<sub>I</sub> (3) = 0.342 nm,  $d_{110}$  I<sub>β</sub> (4) = 0.617 nm,  $d_{110}$  I<sub>β</sub> (5) = 0.538 nm, and  $d_{200}$  I<sub>β</sub> (6) = 0.413 nm. From these *d*-spacings, the unit cell parameters were determined for the *a*- and *b*-axes and monoclinic angle  $\gamma$  for the two phases at 217 °C:  $a = 0.453$  nm,  $b = 0.782$  nm, and  $\gamma = 105.8^\circ$  for cellulose III<sub>I</sub> and  $a = 0.833$  nm,  $b = 0.805$  nm, and  $\gamma = 97.8^\circ$  for cellulose I<sub>β</sub>.

Figure 5 shows the arrangement of molecular chains (*c*-axis projection) and unit cells in the *ab* plane of cellulose III<sub>I</sub> and I<sub>β</sub> at 217 °C. The distance between cellulose chains in a hydrogen-bonded sheet, corresponding to the length of the *b*-axis of cellulose I<sub>β</sub>, is almost the same for the two phases. Furthermore, both crystalline phases have similar intersheet distances; precisely the *d*-spacing (200) of the I<sub>β</sub> phase is a 4.3% smaller than that of the *d*-spacing (110) of III<sub>I</sub> phase. These results suggest the following transformation mechanism. Consider the four types of sheet numbered as 1, 2, 3, and 4 in Figure 5. In the first step of transformation, sheet 1 does not move, but sheets 2, 3, and 4 translate  $+b/4$  in the *b*-axis direction of the I<sub>β</sub> phase. In the next step, sheets 1 and 2 do not move and sheets 3 and 4 translate together  $+b/4$ . Finally, only sheet 4 translates  $+b/4$ . When the sheets translate  $+b/4$  to the *b*-axis direction, they also have to translate  $+c/4$  or  $-c/4$  in the *c*-axis direction. Because the sheets of cellulose I<sub>β</sub> are staggered by  $c/4$  relative to one another, those of cellulose III<sub>I</sub> are not staggered because of the displacement of the one-chain unit cell.<sup>20</sup> For the transformation, all molecular chains also have to rotate approximately  $15^\circ$  about their chain axis, as shown in Figure 5. Cellulose III<sub>I</sub> probably transforms into cellulose I<sub>β</sub> while keeping the sheet structure constant.

The model proposed here was for the case of perfect transformation occurring. In fact, however, cellulose III<sub>I</sub>

transforms into I<sub>β</sub> with reducing crystallite size. This was easily recognized from the broadness of the equatorial peak width of converted cellulose I<sub>β</sub> compared with cellulose III<sub>I</sub> (Figure 4). It has been reported that when cellulose III<sub>I</sub> microcrystals prepared from *Valonia* undergo a transition to cellulose I<sub>β</sub> in hot water, the crystals become subfibrillated into subelements 3–5 nm wide.<sup>13,14</sup> Decrease of crystallite size by the transformation is caused by the fibrillation of microcrystals. Why does the fibrillation occur? One suggestion is that, during the phase translation, a large number of defects are created between the cellulosic sheets due to imperfection of the intersheet sheet translation. Thus, the defects between the sheets might be the beginning of the microcrystalline fibrillation.

## Conclusions

Cellulose III<sub>I</sub> can be transformed into cellulose I<sub>β</sub> by heating above 200 °C without water. With increasing temperature, thermal vibration of the cellulose molecule becomes more active with thermal expansion of the lattice occurs. Breakage of hydrogen bonds may occur at about 200 °C, which could be the trigger for the crystalline phase transformation into cellulose I<sub>β</sub>. At the phase transformation temperature, the intrasheet and intersheet interchain distances is almost the same for both phases. Therefore, an intersheet translation mechanism, in which the sheet structure is retained, is proposed for the phase transformation of cellulose III<sub>I</sub> to cellulose I<sub>β</sub>.

**Acknowledgment.** The author thanks Professor E. Atkins, Dr. J. Hobbs, and Dr. J. Stejny of the University of Bristol for their valuable comments during revised manuscript preparation. This work was supported in part by a Grant-in-Aid for Scientific Research from the Ministry of Education, Science, Sports and Culture, Japan (No. 10760105).

## References and Notes

- (1) Atalla, R. H.; VanderHart, D. L. *Science* **1984**, *223*, 283–285.

- (2) VanderHart, D. L.; Atalla, R. H. *Macromolecules* **1984**, *17*, 1465–1472.
- (3) Sugiyama, J.; Vuong, R.; Chanzy, H. *Macromolecules* **1991**, *24*, 4168–4175.
- (4) Yamamoto, H.; Horii, F.; Odani, H. *Macromolecules* **1989**, *22*, 4130–4132.
- (5) Debzi, E. M.; Chanzy, H.; Sugiyama, J.; Tekely, P.; Excoffier, G. *Macromolecules* **1991**, *24*, 6816–6822.
- (6) Hess, K.; Trogus, C. *Chem. Ber.* **1935**, *68*, 1986–1988.
- (7) Barry, A. J.; Preston, F. C.; King, A. J. *J. Am. Chem. Soc.* **1936**, *58*, 333–337.
- (8) Sarko, A.; Southwick, J.; Hayashi, J. *Macromolecules* **1976**, *9*, 857–863.
- (9) Davis, W. E.; Barry, A. J.; Preston, F. C.; King, A. J. *J. Am. Chem. Soc.* **1943**, *65*, 1294–1299.
- (10) Trogus, C.; Hess, K. *Z. Phys. Chem. (Leipzig)* **1931**, *B14*, 387–395.
- (11) Segal, L.; Loeb, L.; Creely, J. J. *J. Polym. Sci.* **1954**, *13*, 193–206.
- (12) Sueoka, A.; Hayashi, J.; Watanabe, S. *Nippon Kagaku Kaishi* **1973**, 594–602.
- (13) Roche, H.; Chanzy, H. *Int. J. Biol. Macromol.* **1981**, *3*, 201–206.
- (14) Chanzy, H.; Henrissat, B.; Vincendon, M.; Tanner, S. F.; Belton, P. S. *Carbohydr. Res.* **1987**, *160*, 1–11.
- (15) Nishiyama, Y.; Kuga, S.; Wada, M.; Okano, T. *Macromolecules* **1997**, *30*, 6395–6397.
- (16) Yatsu, L. Y.; Calamari, T. A. Jr.; Benerito, R. R. *Textile Res. J.* **1986**, *56*, 419–424.
- (17) Sugiyama, J.; Persson, J.; Chanzy, H. *Macromolecules* **1991**, *24*, 2461–2466.
- (18) Isogai, A.; Usuda, M.; Kato, T.; Uryu, T.; Atalla, R. H. *Macromolecules* **1989**, *22*, 3168–3172.
- (19) Isogai, A.; Usuda, M. *Mokuzai Gakkaishi* **1992**, *38*, 562–569.
- (20) Wada, M.; Heux, L.; Isogai, A.; Nishiyama, Y.; Chanzy, H.; Sugiyama, J. *Macromolecules* **2001**, *34*, 1237–1243.
- (21) Throughout this paper, we used the monoclinic unit cell with dimensions  $a = 0.448$  nm,  $b = 0.785$  nm, and  $c$  (fiber axis) = 1.031 nm;  $\gamma = 105.1^\circ$  as defined in ref 20 for indexing cellulose III<sub>I</sub>.
- (22) Woodcock, C.; Sarko, A. *Macromolecules* **1980**, *13*, 1183–1187.
- (23) The sample weight was found to remain constant either side of this endothermic peak; therefore, it is not due to volatilization of residual ammonia.
- (24) Wada, M.; Okano, T.; Sugiyama, J. *Cellulose* **1997**, *4*, 221–232.

MA0013354